Plasma Atomic Physics

This chapter is devoted to the atomic physics of high-temperature plasmas. We shall assume that temperature is high enough and thus concentration of molecules and molecular ions is negligible. Except for hydrogen, all ions in the plasma may be multiply ionized and various ionization and excitation states may be present. The atomic physics of plasmas has a strong impact on plasma dynamics and it is very important for plasma diagnostics and plasma applications. For the description of plasma dynamics, it is important to know at least the mean ion charge and energy losses due to the emission of radiation. Radiation emitted from the plasma includes very important diagnostic information. Electron temperature, plasma density, and also populations of various ionization states may be determined from the emission spectra. Plasma is a radiation source suitable for many applications. We mention extreme ultraviolet radiation (EUV) with the wavelength 13.5 nm suitable for EUV lithography, which is now used for the production of the most advanced microchips. Radiation with even shorter wavelengths in the water-window region (2.3 - 4.4 nm) is preferable for imaging of biological objects.

1 Charge and excitation states

Roman numbers traditionally denote various charge states. A neutral atom is denoted by I, once ionized by II, twice ionized by III, three times ionized by IV, and so on. As an example, for carbon with atom number $Z_n = 6$ neutral is C I, one time ionized C II, two times ionized C III up to five times ionized carbon C VI. As usually, no excitations of the nucleus are produced in plasmas, we shall not consider states of the bare nucleus (C VII). Spectra of ions with the same number of bound electrons are similar to a certain extent, and thus classification according to the number of bound electrons is also used. Ion C VI has only 1 bound electron, and thus it is also denoted hydrogen-like (H-like) carbon. Similarly, C V is helium-like carbon and C IV is lithium-like carbon.

Each charge state includes a ground state and several excitation states. If only one electron from the outer shell is excited, the state is called a resonance state and its energy is less than the ionization energy of the ground state. Bound states with energy higher than ionization energy are also possible. These states are called autoionization states, as spontaneous ionization from these states is possible when one electron transits to a lower state, and the released energy is transferred to another electron that is moved to continuum. Typically autoionization states originate by excitation of one electron from an inner shell or by excitation of 2 electrons from the outer shell.

Simple schematics of energy levels is demonstrated in Figure 1. Fine splitting of levels of hydrogen-like may be usually disregarded, the state can be assumed one state with degeneracy $g = 2n^2$. For multi-electron ions, splitting of the level has to be taken into account. Splitting for lighter elements is usually according to LS coupling, while jj coupling is usual for heavier elements. Energy levels are split in LS coupling according to total orbital angular momentum L and total spin angular momentum S. The ground state of a helium-like ion has both electrons in the completely filled K-shell, and thus has L = S = 0 and this state is denoted $1s^2\ ^1S$, where S means L = 0 and upper index 1 means singlet state (S = 0). Resonance excited states are 1snl and are split according to L and S. The first excited state contains configurations 1s2s and 1s2p, and the value of total spin angular momentum S can be 0 or 1. The first excited state of helium-like ion is split into 4 levels: 1s2s ^{1}S with weight (degeneracy) $g = 1$, 1s2s ^{3}S with $g = 3$, 1s2p ^{1}P with $g = 3$ and 1s2p ^{3}P with $g = 9$. Here, P denotes L = 1, upper index is determined

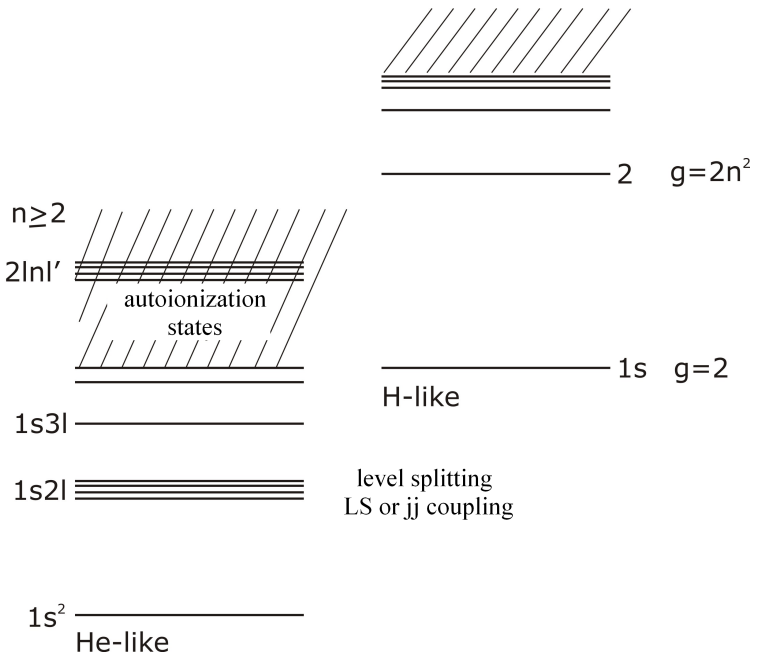

Figure 1: Schematics of energy levels of helium-like and hydrogen-like ions.

by $2k+1$ possible orientations of total spin angular momentum k. Degeneration g is given by the product of the possible orientations of orbital and spin angular momentum. The magnitude of energy splitting usually decreases for higher energy levels.

The strongest lines in the emission spectrum usually belong to resonant transitions that are allowed dipole transitions between atomic states. For LS coupling there exist restrictions for resonant radiative transitions: the total spin angular momentum cannot change $\Delta S = 0$ and the total orbital angular momentum can change only by $\Delta L = \pm 1$, or alternatively, it may be $\Delta L = 0$ when $L \neq 0$. The transitions that do not meet the above conditions are forbidden and transition probability is usually substantially lower.

Detailed simulations of plasma atomic physics are composed of 2 parts. In the first one, the structure of electron cloud in atom is modeled and energy levels, wave functions and transition probabilities are calculated. In the second part, populations of ionization and excitation are calculated for known density, temperature, and size of plasma or for known history of these parameters. External sources of radiation can also be taken into consideration. Then emission or absorption spectra may be also synthesized. This second task can also be solved as a post-processor to fluid simulation of plasma dynamics.

2 Atom's electron shell structure

The atomic structure is fully consistently described by the relativistic Dirac equation [1]. However, we will use a simpler approach using the non-relativistic Schrödinger equation with relativistic corrections. We will follow the book [2].

When describing the electron shell of an atom, we will normalize the spatial coordinates to the Bohr radius a_0

$$a_0 = \frac{4\pi\varepsilon_0\hbar^2}{m_e e^2} = 5.29177 \times 10^{-11}\ \mathrm{m} \tag{1}$$

and energies will be normalized to the Rydberg constant R_∞ (Ry)

$$1 \text{ Ry} = R_\infty = \frac{e^2}{8\pi\varepsilon_0 a_0} = \frac{e^4 m_e}{2(4\pi\varepsilon_0\hbar)^2} = 13.6058 \text{ eV} = 109737 \text{ cm}^{-1} \ . \tag{2}$$

Here e is the elementary charge, m_e is the mass of the electron, Planck's constant $\hbar = h/(2\pi)$ and ε_0 is the permittivity of free space. The energy unit cm^{-1} is used in spectroscopy, it is the inverse wavelength of a photon with a given energy.

2.1 One-electron atom (ion)

The electron moves in the central electrostatic field $V(r)$ of the nucleus and its energy E is the eigenvalue of the Hamilton operator. The wave function of the electron is obtained by solving the time-independent Schrödinger equation

$$\mathbf{H}\varphi = E\varphi \tag{3}$$

$$\begin{aligned} \mathbf{H} &= \frac{p^2}{2m_e} + V(r) = \frac{p_r^2}{2m_e} + \frac{\mathbf{L}^2}{2m_e} + V(r) = \\ &= -\frac{\hbar^2}{2m_e}\left[\frac{1}{r}\frac{\partial^2}{\partial r^2}r + \frac{1}{r^2\sin\theta}\left(\frac{\partial}{\partial\theta}\sin\theta\frac{\partial}{\partial\theta}\right) + \frac{1}{r^2\sin^2\theta}\frac{\partial^2}{\partial\phi^2}\right] + V(r) \ , \end{aligned}$$

where the potential of a nucleus with atomic number Z is $V(r) = -Ze^2/(4\pi\varepsilon_0 r)$. If we measure distances in Bohr radii a_0 and energies in Rydberg units (Ry), then the timeless Schrödinger equation becomes

$$\left[-\frac{1}{r}\frac{\partial^2}{\partial r^2}r + \frac{\mathbf{L}^2}{r^2} - \frac{2Z}{r}\right]\varphi = E\varphi \ . \tag{4}$$

In any central field problem, the angular momentum $\mathbf{L}$ is a constant of motion. In quantum mechanics, we would expect the wave function φ to be an eigenfunction of the operators $\mathbf{L}^2$, $\mathbf{L}_z$. This is indeed true, since $\mathbf{L}^2$ is the only term in the Schrödinger equation that depends on θ and ϕ.

The solution can then be written in the form

$$\varphi(\vec{r}) = \varphi_{nlm_l m_s}(\vec{r}) = \frac{1}{r}P_{nl}(r)\cdot Y_{lm_l}(\theta,\phi)\cdot\sigma_{m_s}(s_z) \ , \tag{5}$$

where $n = 1, 2, \ldots$ is the principal quantum number, $l = 0, 1, \ldots, n-1$ characterizes the orbital angular momentum, $m_l = -l, -l+1, \ldots, l-1, l$ is the orientation of the orbital angular momentum and $m_s = -1/2, 1/2$ is the orientation of the spin angular momentum.

All angular momentum operators have the following properties (here we give them for an arbitrary angular momentum J). The operator $\mathbf{J}^2 = \vec{\mathbf{J}}\cdot\vec{\mathbf{J}} = \mathbf{J}_x^2 + \mathbf{J}_y^2 + \mathbf{J}_z^2$ has eigenvalues $j\,(j+1)\,\hbar^2$, where $j = 0, 1/2, 1, 3/2, 2, \ldots$ and J_z has eigenvalues $m\hbar$ ($m = -j, -j+1, -j+2, \ldots, j-1, j$). The orientations of the angular momentums are schematically shown in Fig.2

The eigenfunctions of the orbital angular momentum operators $\mathbf{L}^2$, $\mathbf{L}_z$ are spherical harmonics

$$Y_{lm}(\theta,\phi) = \Theta_{lm}(\theta)\Phi_m(\phi) = (-1)^{(m+|m|)/2}\left[\frac{(2l+1)(l-|m|)!}{4\pi(l+|m|)!}\right]^{1/2} P_l^{|m|}(\cos\theta)\exp(im\phi) \ . \tag{6}$$

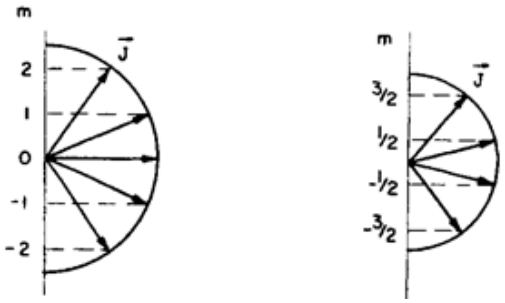

Figure 2: Semiclassical scheme for angular momenta J = 2 and 3/2 (taken from [2]).

Spherical harmonics are orthonormal and their sum over m

$$\sum_{m=-l}^{l} |Y_{lm}(\theta,\phi)|^2 = \frac{2l+1}{4\pi}$$

is spherically symmetric. This results in spherical symmetry of the electron density in any fully occupied subshell. States with angular momentum $l = 0$ are denoted by s, p denotes $l = 1$, d ($l = 2$), f ($l = 3$), g ($l = 4$), h ($l = 5$), i ($l = 6$), k ($l = 7$), l ($l = 8$), m ($l = 9$).

The electron has its own angular momentum - spin $j = 1/2$ (the z component is $m_s = -1/2, 1/2$), the eigenfunction is $\sigma_{m_s}(s_z) = \delta_{m_s s_z}$. States with differences in quantum numbers are orthonormal $\left\langle Y_{lm_l}\sigma_{m_s}|Y_{l'm'_l}\sigma_{m'_s}\right\rangle = \delta_{ll'}\delta_{m_l m'_l}\delta_{m_s m'_s}$.

2.1.1 Radial part of the wave function

The wave function is zero at the location of nucleus $P_{nl}(0) = 0$. For free states ($E_{\bar{e}l} > 0$), the open boundary condition at $r \to \infty$ leads to a continuous energy spectrum. For bound states ($E_{nl} < 0$) only discrete energy levels are allowed, since the wave function must go to 0 for $r \to \infty$. The equation for the radial part of the wave function is

$$\left[-\frac{\mathrm{d}^2}{\mathrm{d}r^2} + \frac{l(l+1)}{r^2} - \frac{2Z}{r}\right] P_{nl}(r) = E P_{nl}(r) \ . \tag{7}$$

Here the effective potential is $V_{eff}(r) = V(r) + l(l+1)/r^2 = -2Z/r + l(l+1)/r^2$. After substituting $\rho = 2Zr/n$ and $E = -Z^2/n^2$ the equation is transformed to the form

$$\left[\frac{\mathrm{d}^2}{\mathrm{d}\rho^2} - \frac{1}{4} + \frac{n}{\rho} - \frac{l(l+1)}{\rho^2}\right] P_{nl}(\rho) = 0 \ . \tag{8}$$

The analytical solution of the equation is as follows

$$P_{nl}(\rho) = -\left[\frac{Z(n-l-1)!}{n^2(n+l)!^3}\right] \rho^{l+1} \mathrm{e}^{-\rho/2} \mathrm{L}_{n+l}^{2l+1}(\rho) \ , \tag{9}$$

where the associated Laguerre polynomial is

$$\mathrm{L}_{n+l}^{2l+1}(\rho) = -(n+l)!^2 \sum_{k=0}^{n-l-1} \frac{(-\rho)^k}{k!(n-l-1-k)!(2l+1+k)!} \ .$$

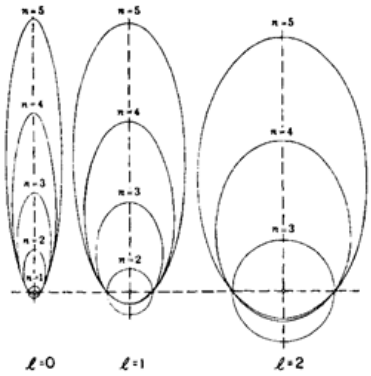

Figure 3: Eliptical Bohr-Sommerfeld orbits for hydrogen atom (taken from [2]).

The phase of the general solution is arbitrary, here we use the convention $P_{nl}(r) > 0$ for $r \to 0$. The number of nodes (zeros) is $n - l - 1$, the number of extrema is $n - l$.

Bohr-Sommerfeld orbits have an elliptical shape. The orbit with $l = n - 1$ is spherical, with increasing n the orbits for a given l become more and more elongated in the direction of the major axis. The maximum distance from the nucleus increases, but the closest point to the nucleus gets closer. The closer an electron in the s state with a high principal quantum number n approaches the nucleus, the greater its binding energy and leads to an anomaly for neutral atoms, when the s state with a higher principal quantum number is occupied earlier than the d and f states with a lower principal quantum number. This anomaly also exists for some once and twice ionized ions of heavy elements, but never occurs for higher degrees of ionization.

For atoms and ions with multiple bound electrons, the effective potential does not have an analytically explicit form and an analytical solution for the wave function cannot be found. In the numerical solution, the energy value is iterated and the number of nodes must correspond to the respective state.

2.1.2 Relativistic corrections

In order to achieve qualitative and quantitative agreement with the observed splitting of spectral lines and transition energies, it is necessary to add relativistic corrections to the Hamiltonian, which then has the form [2]

$$\mathbf{H} = -\nabla^2 + V - \frac{\alpha^2}{4}(E - V)^2 - \frac{\alpha^2}{4}\left(\frac{\mathrm{d}V}{\mathrm{d}r}\right)\frac{\partial}{\partial r} + \frac{\alpha^2}{2r}\left(\frac{\mathrm{d}V}{\mathrm{d}r}\right)\left(\vec{\mathbf{l}}\cdot\vec{\mathbf{s}}\right) \ , \tag{10}$$

where the fine structure constant $\alpha = e^2/(4\pi\varepsilon_0\hbar c) = \hbar/(m_e c a_0) = 1/137.036$ and $V = -2Z/r$ for hydrogen-like ions. The third term of the Hamiltonian is the mass-velocity term given by the dependence of the electron mass on its velocity. The fourth term is the so-called Darwin term expressing the relativistic correction due to the uncertainty of the electron position. The last term is the spin-orbital term caused by the magnetic interaction of the orbital and spin magnetic momenta. While the mass-velocity and Darwin terms lead only to a shift of energy levels, the spin-orbital coupling leads to a splitting of energy levels with $l \neq 0$.

The operator $\vec{\mathbf{l}}\cdot\vec{\mathbf{s}} = \left(\mathbf{j}^2 - \mathbf{l}^2 - \mathbf{s}^2\right)/2$ has eigenvalues $X = [j(j+1) - l(l+1) - s(s+1)]$, which can be simplified to $X = l$ for $j = l + 1/2$ and $X = -l - 1$ for $j = l - 1/2$. The radial part of the wave function depends on the quantum numbers n, l and, newly, j and can be calculated directly from the radial part of the Schrödinger equation. The energy corrections can

be calculated from the classical $P_{nl}(r)$ using the relativistic correction terms of the Hamiltonian. The energy shift due to spin-orbital coupling is then given by

$$\delta E_{so} = \alpha^2 Z X \left\langle r^{-3} \right\rangle = (1-\delta_{l0}) \frac{\alpha^2 Z^4}{n^3 l(l+1)(2l+1)} \left[j(j+1) - l(l+1) - s(s+1) \right] \ . \qquad (11)$$

All relativistic energy corrections are proportional to Z^4 and thus grow with Z faster than the fundamental terms proportional to Z^2.

3 Many-electron atom (ion)

We will not consider the terms mass-velocity and Darwin for now because their influence on the energies of the states can be calculated additionally using the perturbation method. However, we must include the spin-orbit coupling, as it significantly influences the structure of the energy levels. We will therefore solve the Schrödinger equation with a Hamiltonian of the form

$$\mathbf{H} = \mathbf{H}_{kin} + \mathbf{H}_{e-nuc} + \mathbf{H}_{e-e} + \mathbf{H}_{so} = -\sum_i \nabla_i^2 - \sum_i \frac{2Z}{r_i} + \sum_i \sum_{j<i} \frac{2}{r_{ij}} + \sum_i \xi_l(r_i) \left(\vec{\mathbf{l}}_i \cdot \vec{\mathbf{s}}_i \right) \ . \qquad (12)$$

The multiplication factor ξ_l can be calculated from the knowledge of the used approximate or self-consistent potential of the fields $V(r)$ using the relation $\xi_l = \alpha^2/2r \times (\mathrm{d}V/\mathrm{d}r)$.

The wave functions $\Psi^k(\vec{r})$ of complex atoms are solutions of the Schrödinger equation and are expressed as linear combinations of basis functions ψ_b

$$\mathbf{H}\Psi^k(\vec{r}) = E^k \Psi^k(\vec{r}) \qquad \Psi^k(\vec{r}) = \sum_b y_b^k \psi_b \ . \qquad (13)$$

Basis functions are orthonormal and form a complete system of functions. In general, this system is infinite.

Basis functions are constructed from the one-electron wave functions $\varphi_i(\vec{r}_i)$. The Pauli exclusion principle requires basis functions to be antisymmetric concerning the exchange of any 2 electrons. Such functions can be constructed in the form of determinants

$$\psi_b = (N!)^{-1/2} \sum_P (-1)^p \varphi_1(\vec{r}_{j_1}) \varphi_2(\vec{r}_{j_2}) \dots \varphi_N(\vec{r}_{j_N}) \ , \qquad (14)$$

where $p = 0$ for even permutation and $p = 1$ for odd permutation and $\vec{r}$ also includes the spin $\vec{s}$. The antisymmetrized function eliminates the possibility that any two orbitals are identical, as this would lead to $\psi_b = 0$. Furthermore, electrons with the same spin cannot be in the same place, so ψ_b must be very small when electrons with the same spin are close to each other. Thus, antisymmetrized basis wave functions include correlations of electrons with the same spin via the Pauli exclusion principle. Conversely, electrons with opposite spins are not correlated, since the basis functions contain no correlation due to Coulomb repulsion.

Electrons with the same n and l form a subshell and are called equivalent electrons. A list of N pairs $n_i l_i$ defines a configuration. If the number of electrons in a subshell k is denoted by w_k, then the configuration is specified by the following notation

$$(n_1 l_1)^{w_1} (n_2 l_2)^{w_2} \dots (n_h l_h)^{w_h} \ , \quad \text{where} \ \sum_{k=1}^{h} w_k = N \ .$$

A fully occupied subshell k (s^2, p^6, d^{10}, $f^{14}, \dots$) is called closed and its angular momenta $L_k = S_k = J_k = 0$. Closed subshells are usually omitted in shorthand notation, so the configuration Ne I $1s^2 2s^2 2p^5 3s$ is written Ne I $2p^5 3s$.

3.1 Energy averaged over configuration and radial wave functions

The energy E_{av} averaged over a configuration is the mean value of the energy of the set of all basis functions belonging to a given configuration, i.e., all allowed combinations of orbital and spin angular momenta of all electrons. It is expressed as

$$E_{av} = \langle b|\mathbf{H}|b\rangle_{av} = \sum_b \langle b|\mathbf{H}|b\rangle /M = \sum_b E^b/M \ ,$$

where M is the number of basis functions. E_{av} is also the energy of a spherically centered atom. The spin-orbital contributions to E_{av} cancel each other out due to the presence of functions with spins $\pm 1/2$.

The contribution of interactions between electrons consists of a direct and exchange term, the energy centered over the configuration is thus expressed as

$$E_{av} = \sum_i \left\langle i|-\nabla^2|i\right\rangle_{av} - \sum_i \left\langle i|\frac{2Z}{r_1}|i\right\rangle_{av} + \sum_i \sum_{j<i} \left[\left\langle ij|\frac{2Z}{r_{12}}|ij\right\rangle_{av} - \left\langle ij|\frac{2Z}{r_{12}}|ji\right\rangle_{av}\right] \ , \quad (15)$$

where the first term is the sum of the kinetic energies of the electrons centered over the configuration, the second term is the sum of the potential energies centered in the nuclear field, and the third term is given by the mutual potential energies E_{ij}. The binding energy of the ith electron in the state $n_i l_i$ centered over the configuration is

$$E^i = E^i_k + E^i_n + \sum_{j\neq i} E^{ij} \ ,$$

where E^i_k is the kinetic energy, E^i_n is the potential energy in the nuclear field, and E^{ij} is the mutual potential energy between the i-th and j-th electrons. The total binding energy therefore differs from the sum of the binding energies of all electrons by one half of the sum of the mutual potential energies E^{ij}.

The radial wave functions $P_{n_j l_j}$ are identical for all electrons in a subshell. These functions minimize the atom's energy centered over the configuration while satisfying the orthonormality binding condition for the functions with different n and the same l.

The radial wave functions are solutions of the self-consistent Hartree-Fock (HF) equation

$$\left[-\frac{\mathsf{d}^2}{\mathsf{d}r^2} + \frac{l_i(l_i+1)}{r^2} - \frac{2Z}{r} + \sum_{j=1}^{q}(w_j - \delta_{ij})\int_0^\infty \frac{2}{r_>}P_j^2(r_2)\mathsf{d}r_2 - (w_i-1)A_i(r)\right] P_i(r) =$$

$$= \varepsilon_i P_i(r) + \sum_{j=1(j\neq i)}^{q} w_j \left[\delta_{l_i l_j}\varepsilon_{ij} + B_{ij}(r)\right] P_j(r) \ . \quad (16)$$

Here $r_> = \max(r, r_2)$, A_i, B_{ij}, expressed by integrals P_i, P_j are the exchange potential energies in one subshell and in different subshells. The fourth term on the left is the potential energy $V^i_H(r)$ of the ith electron in a spherically centered field of the other $(N-1)$ electrons. The Lagrange multipliers ε_{ij} are changed so as to achieve orthogonality of the functions P. The multipliers ε_i express the binding energy of the electron in the subshell

$$\varepsilon_i = E^i_k + E^i_n + \sum_{j(\neq i)=1}^{N} E^{ij} = E^i \ . \quad (17)$$

The HF equation is then solved by iteration of the self-consistent field (SCF iteration). This iteration has difficulty converging for high orbits of neutral and lowly ionized atoms. For integrals with P_i in the denominator, other methods of calculating radial wave functions are preferred due to the zeros of P_i.

There are several approximate methods for calculating radial wave functions and binding energies. All of them use local potentials, they are spared the complexity of SCF iteration, and are suitable for calculating integrals. The Thomas-Fermi (TF) and Thomas-Fermi-Dirac (TFD) methods, which is TF with an added exchange potential, use an atom with half-free electrons. They are simple, but the potential used is poor. The Hartree method uses $V(r) = -2Z/r + V_H(r)$, the disadvantage being the absence of exchange terms. In the Hartree-Fock-Slater (HFS) method, exchange effects are included in the same way as in the TFD method. The most accurate known is the frequently used HX (Hartree-plus-Statistical-Exchange) method. The potential has the form $V_i(r) = -2Z/r + V_H(r) + V_x(r)$, where $V_x(r)$ is an approximation for the exchange terms based on a statistical approach.

3.2 Detail structure of energetic levels

The splitting of energy levels within a configuration is caused by the coupling of angular momentum. The composite function of two angular momenta is expressed using the Clebsch-Gordon coefficients C as follows

$$|j_1 j_2 jm\rangle = \sum_{m_1=-j_1}^{j_1} C(j_1 j_2 m_1, m-m_1; jm)\, |j_1 j_2 m_1, m-m_1\rangle = (-1)^{j_1+j_2-j}\, |j_2 j_1 jm\rangle \ . \quad (18)$$

It is eigenfunction of 4 operators $\mathbf{J}_1^2$, $\mathbf{J}_2^2$, $\mathbf{J}^2 = (\mathbf{J}_1 + \mathbf{J}_2)^2$ $\mathbf{J}_z = \mathbf{J}_{1z} + \mathbf{J}_{2z}$. Adding two angular momenta is not commutative. Adding three angular momenta is even more complicated and is not associative.

The basic splitting of the energy levels is influenced by the relative importance of the different terms of the Hamiltonian. We describe here two basic schemes - **LS** coupling and **jj** coupling. Some configurations behave according to other schemes (**LK** coupling, **jK** coupling) and other configurations have an intermediate coupling, which means that they cannot be assigned to any general coupling scheme.

LS coupling is characteristic for atoms with low Z, where the Coulomb repulsion dominates the spin-orbital interaction. The basic splitting is according to the total orbital angular momentum $\mathbf{L} = \sum_i \vec{\mathbf{l}}_i$ and according to the total spin $\mathbf{S} = \sum_i \vec{\mathbf{s}}_i$. Then $\mathbf{L}$ and $\mathbf{S}$ are combined to form the eigenfunctions $\mathbf{J}^2$, $\mathbf{J}_z$. The usual notation for the states is $^{2S+1}\mathsf{L}_\mathsf{J}$, where $2S+1$ is the multiplicity due to the possible orientations of the total spin, the total orbital angular momentum L is represented by the letters S, P, D,... for $L = 0, 1, 2, \ldots$, and odd parity is denoted by the superscript o, for example $^3\mathrm{S}_1$, $^2\mathrm{P}^o_{1/2}$.

Conversely, elements with high Z, where spin-orbit interaction dominates over electrostatic repulsion, behave according to **jj** coupling. Here, the orbital and spin angular momentum for each electron are first summed $\vec{\mathbf{l}}_i + \vec{\mathbf{s}}_i = \vec{\mathbf{j}}_i$, and then the total angular momentum is summed together. The level designation for 2 electrons is $[(l_1, s_1)\, j_1, (l_2, s_2)\, j_2]\, \mathbf{JM}$.

The scheme of splitting the energy levels of the ***pd*** configuration for **LS** and **jj** coupling is demonstrated in Fig. 4. Both schemes start from an energy E_{av} centered over the configuration. The **LS** coupling gradually adds a large Coulomb interaction (direct and exchange), a spin-orbit interaction, and finally the influence of an external magnetic field. In the **jj** coupling, 2 strong spin-orbit interactions lead to 4 energies; the small Coulomb interaction then leads to a small splitting according to the total angular momentum **J**.

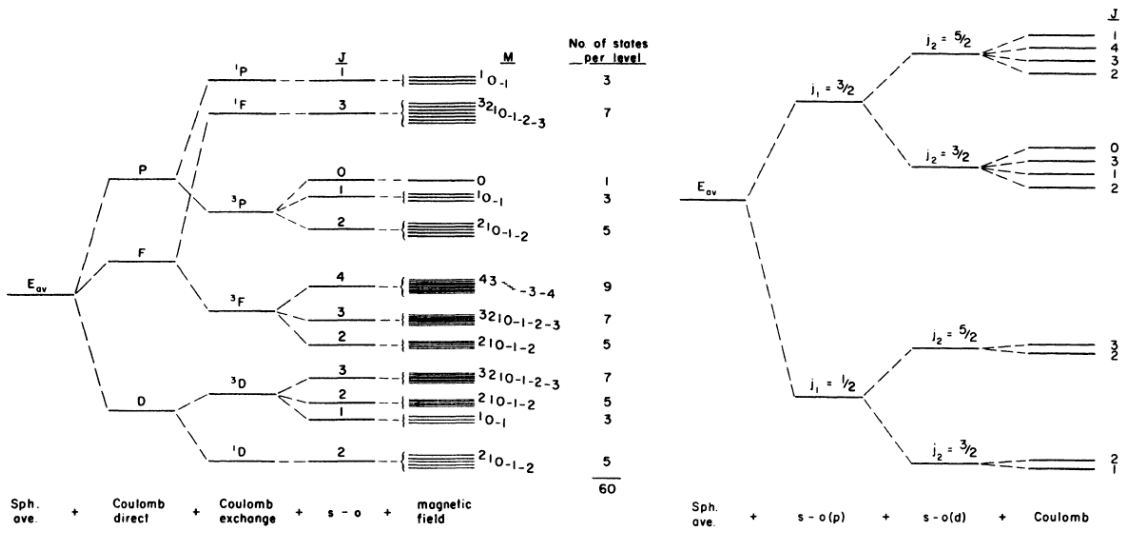

Figure 4: Splitting of ***pd*** configuration for **LS** coupling (left pannel) and for **jj** coupling (right pannel) (taken from [2]).

4 Atomic processes

The effective cross sections and rate coefficients of individual atomic processes can be calculated precisely from knowledge of the final and initial state wave functions. However, we will focus here on simple approximate relationships that demonstrate the qualitative characteristics of individual processes.

Atomic processes are usually divided into collisional processes (processes without the participation of a photon) and radiative processes.

4.1 Collisional processes

For the process α, where particles 2 are hit by a flow of $\Gamma_1 = n_1 g$ of particles 1 (g is the mutual velocity), the effective cross section $Q^{(\alpha)}$ is given by the number of events per unit time per particle of type 2 divided by the flow Γ_1 of incoming particles 1. The number of events α per unit time in a unit volume is

$$R_{12}^{(\alpha)} = n_1 n_2 g Q_{12}^{(\alpha)}(g) \qquad \left(R_{11}^{(\alpha)} = \frac{1}{2} n_1^2 g Q_{11}^{(\alpha)}(g) \right) \tag{19}$$

The reduction in the number of particles n_2 in a unit volume by the process α is given by the relation

$$\left(\frac{\mathrm{d}n_2}{\mathrm{d}t} \right)^{(\alpha)} = -R_{12}^{(\alpha)}$$

Unless the density of free electrons is small compared to the density of other particles, collisions of ions with electrons dominate.

4.1.1 Collisional excitation (de-excitation)

We will describe the excitation from a lower level k to a higher level l

$$i^{(k)} + e \rightleftarrows i^{(l)} + e \qquad \varepsilon_{kl} = \varepsilon_l - \varepsilon_k$$

The threshold energy of an electron for excitation is ε_{kl}. For collision processes, selection rules do not apply and collision excitation for a forbidden transition can have a similar probability as for an allowed transition. Usually, the effective cross section increases rapidly above the threshold energy ε_{kl}, reaches a maximum at several times the threshold energy, and then decreases. For allowed dipole transitions, an approximate formula for the effective cross section of collision excitation [3] can be written as a function of the ratio $u = \varepsilon/\varepsilon_{kl}$ of the energy ε of the incident electron to the threshold energy ε_{kl}

$$Q^{(k\to l)}(\varepsilon) = 4\pi a_0^2 \left(\frac{\varepsilon^H}{\varepsilon_{kl}}\right)^2 f_{kl}\beta_1 g(u) \ , \tag{20}$$

where $a_0 = 4\pi\varepsilon_0\hbar^2/(m_e e^2) = 5.3 \times 10^{-11}$ m is the Bohr radius, $\varepsilon^H = 13.6$ eV is the ionization potential of the hydrogen atom, f_{kl} is the oscillator strength for absorption and the functions

$$g(u) = \frac{u-1}{u^2} \ln\left(1.25\beta_2 u\right)$$

and β_1, β_2 are constants of order 1. The function $g(u)$ shown in Fig. 5 attains a maximum for $u \simeq 2$ - 4.

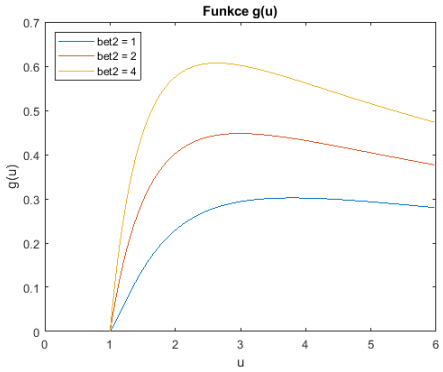

Figure 5: Function g for different β_2 depending on the ratio u of the energy ε of the electron to the threshold energy ε_{kl}.

The effective cross section $Q \sim \varepsilon_{kl}^{-2}$, and therefore collision processes are fast between nearby levels. For example, collision processes can ensure equilibrium within a single split level of a given configuration. Equilibrium will be better ensured at higher levels, where the energy splitting is smaller.

4.1.2 Collisional ionization (three-particle recombination)

We describe the ionization of an atom (ion) Y from level k

$$Y + e \rightleftarrows Y^+ + e + e \ \ ,$$

where the ionization energy from level k is $\varepsilon_{k\lambda}$. Let the energy of the incident electron be ε. We denote $u = \varepsilon/\varepsilon_{k\lambda}$. The effective collision ionization cross section is then

$$Q^{(k\to\lambda)}(\varepsilon) = 2.66\pi a_0^2 \left(\frac{\varepsilon^H}{\varepsilon_{k\lambda}}\right)^2 \xi_k\beta_1 g(u) \ , \tag{21}$$

where ξ_k is the number of electrons in the outer shell at level k. Again, the dependence of the effective cross section for ionization on the ratio u of the electron energy ε to the threshold energy $\varepsilon_{k\lambda}$ is given by the function $g(u)$ mentioned above. The effective cross section is inversely proportional to the square of the threshold energy and is therefore larger for higher excited states with small ionization potential. The rate of three-particle recombination is proportional to $n_i n_e^2$ and is therefore non-negligible only in dense plasmas.

4.1.3 Dielectron recombination

Dielectron recombination is a two-step collision-radiation process. If an ion Y^+ captures a free electron, an autoionization state Y^{**} of the atom (ion) Y with an energy higher than its ionization potential I_p is created. By emitting a photon, the atom (ion) goes into the excited state Y^*. The process scheme is

$$Y^+ + e \longrightarrow Y^{**} \longrightarrow Y^* + h\nu \ .$$

The rate of dielectron recombination is proportional to $n_+ n_e$, and in less dense plasmas it may dominate over three-particle recombination.

4.2 Radiation processes

Radiation processes can be divided into three groups according to the nature of the initial and final states.

1. Bound – bound transitions (photodeexcitation and photoexcitation) correspond to the line spectrum of radiation.

2. Free – bound transitions (photorecombination and photoionization) correspond to continuous radiation with a minimum photon energy (recombination edge).

3. Free – free transitions (bremsstrahlung and collisional absorption) correspond to the unbounded continuous spectrum.

Here we will assume that the photon frequency is much larger than the electron plasma frequency ω_{pe}, and therefore we can set the relative permittivity $\varepsilon_r = 1$ with good accuracy.

4.2.1 Bound – bound transitions

These are photodeexcitation processes, when an ion (atom) goes from a higher state l to a lower state k and the energy difference is emitted in the form of a photon, and the inverse process of photoexcitation. Schematically, they can be written

$$i^{(l)} \rightleftarrows i^{(k)} + h\nu \qquad h\nu = \varepsilon_l - \varepsilon_k \qquad \vec{p}_\nu = \frac{h\nu}{c}\vec{\Omega} \ \ ,$$

where $\vec{\Omega}$ is the unit vector in the direction of photon propagation.

The intensity of radiation in the infinitesimal spectral and angular region is $I_\nu(\vec{\Omega})\mathrm{d}\nu\mathrm{d}\vec{\Omega}$, where the quantity $I_\nu(\vec{\Omega})$ is called the spectral intensity of radiation. For an isotropic electromagnetic field,

$$I_\nu(\vec{\Omega}) = n_\nu \frac{c}{4\pi} h\nu \ \ ,$$

where n_ν is the volume density of photons in the given spectral region.

The number of photons absorbed by stationary particles of concentration n_k in unit volume per unit time is

$$R = \int R_\nu \mathrm{d}\nu = n_k \int \frac{I_\nu(\vec{\Omega})}{h\nu} \mathrm{d}\nu Q_\nu \mathrm{d}\vec{\Omega} \ ,$$

where Q_ν is the effective cross section for absorption. In the case of moving particles, ν varies due to the Doppler effect, and in a laboratory system the effective cross section depends on the particle velocity vector and the direction of radiation propagation. The effective cross section for photoexcitation for an allowed dipole transition is

$$Q_\nu^{(k\to l)} = \frac{e^2}{4\varepsilon_0 m_e c} f_{kl} \Phi(\nu) \quad , \tag{22}$$

where f_{kl} is the oscillator strength for absorption (usually $0 < f_{kl} < 1$) and $\Phi(\nu)$ is the shape of the absorption line ($\int \Phi(\nu)\mathrm{d}\nu = 1$). The shape of the emission line is usually the same as that of the absorption line, but in some situations it can be different. The oscillator strength f_{lk} for emission is also introduced, which is negative and holds $f_{lk} = -g_k f_{kl}/g_l$ and where g denotes the degeneracy of the respective state.

To calculate the number of absorbed photons in a unit volume per unit time, it is necessary to integrate the radiation intensity over frequency and over solid angle

$$I^{kl}(\vec{\Omega}) = \int I_\nu(\vec{\Omega})\Phi(\nu)\mathrm{d}\nu \qquad\qquad \overline{I}^{kl} = \int I^{kl}(\vec{\Omega})\mathrm{d}\vec{\Omega} \ .$$

If the radiation intensity changes slowly, we can set $I^{kl}(\vec{\Omega}) \simeq I_{\nu_{kl}}$. If we compare the number of photoexcitations from state k to state l per unit volume per unit time expressed in terms of the effective cross section with the expression using Einstein's coefficient B_{kl} for absorption, we get the value of the Einstein coefficient

$$R^{kl} = n_k \frac{\overline{I}^{kl}}{h\nu} \frac{e^2}{4\varepsilon_0 m_e c} f_{kl} = n_k B_{kl} \overline{I}^{kl} \qquad \Longrightarrow \qquad B_{kl} = \frac{e^2}{4\varepsilon_0 m_e c h \nu_{kl}} f_{kl} \tag{23}$$

The number of photons emitted by stimulated emission per unit volume per unit time is expressed using Einstein's coefficient B_{lk} for stimulated emission

$$R^{lk}_{stim} = n_l B_{lk} \overline{I}^{kl} \tag{24}$$

Spontaneous emission rate R^{lk}_{stim} and radiative lifetime τ_{lk}

$$R^{lk}_{spon} = n_l A_{lk} \qquad\qquad \tau_{lk} = A_{lk}^{-1} \ , \tag{25}$$

where A_{lk} is the Einstein coefficient for spontaneous emission.

The relationships between Einstein coefficients can be derived from the conditions for thermodynamic equilibrium, where the number of photons emitted at the transition $l \to k$ must equal the number of photons absorbed at the transition $k \to l$ and the populations of states are given by

$$n_k = \frac{g_k}{g_l} n_l \mathrm{e}^{h\nu/k_B T} \ .$$

From here we express the spectral intensity of the radiation and compare it with the Planck spectrum of blackbody

$$I^{kl}_\nu = \frac{\overline{I}^{kl}_\nu}{4\pi} = \frac{A_{lk}/(4\pi)}{\frac{g_k}{g_l} B_{kl} \mathrm{e}^{h\nu_{kl}/k_B T} - B_{lk}} = B_\nu = \frac{2h\nu^3/c^2}{\mathrm{e}^{h\nu/k_B T} - 1} \ .$$

From here we obtain the following relations for the Einstein coefficients

$$g_k B_{kl} = g_l B_{lk} \qquad \frac{A_{lk}}{B_{lk}} = \frac{8\pi h\nu_{kl}^3}{c^2} \implies A_{lk} = \frac{g_k}{g_l}\frac{2\pi e^2 \nu_{kl}^2}{\varepsilon_0 m_e c^3} f_{kl} \ . \tag{26}$$

The spontaneous emission coefficient is proportional to the square of the photon frequency, and the allowed dipole transitions are therefore fast for a large energy difference between states, which is the opposite of collision processes, which are fast between states of similar energy. The typical lifetime for a strong dipole transition in the optical region with a photon energy of ∼1 eV is 10 - 100 ns, but in the XUV (soft X-ray) region with a photon energy of ∼1 keV it is $10^6\times$ shorter (10 - 100 fs). The emission and absorption lines very often have the same shape $\Phi(\nu)$. This function is never a δ function, but the spectral line is broadened by various processes.

1. Natural broadening - due to spontaneous emission the lifetime of the energy state is finite and due to the Heisenberg uncertainty relation $\delta(E) \times \delta(t) \geq \hbar/2$ has a finite width of energy. The width of the transition from state l to state k is

$$\Delta\varepsilon_{jk} = h\gamma_{lk} \qquad \gamma_{lk} = \gamma_l + \gamma_k \qquad \gamma_l = \sum_{j<l} A_{lj} \ .$$

   The spectrum corresponds to a damped oscillator with natural frequency ν_{kl} and damping coefficient γ_{lk}. This spectrum is given by the Lorenz line shape

$$\Phi(\nu) = \frac{1}{\pi}\frac{\gamma_{lk}/4\pi}{(\nu-\nu_{kl})^2 + (\gamma_{lk}/4\pi)^2} \tag{27}$$

   The natural broadening is usually smaller than other types of broadening (except for very rarefied systems with low ion temperatures).

2. Pressure broadening - is a consequence of the interaction of the emitter with the surrounding particles. In a plasma with a predominance of charged particles, the pressure broadening is given by the action of electric fields on the emitter, so it is called Stark broadening. It is due to collisions with free electrons (impact broadening) and due to quasi-stationary ion microfields. For neutral particles, for example, Van der Waals broadening occurs.

3. Doppler broadening - due to the thermal motion of ions in the direction of emission, the emission frequencies of individual ions are shifted by the Doppler effect. The line profile depends on the partition function of the emitting ions. For the Maxwell's distribution, the line profile has the form

$$\Phi(\nu) \sim \exp\left[-\frac{(\nu-\nu_{kl})^2}{\Delta\nu_D^2/4\ln 2}\right] \tag{28}$$

   If both Lorentz and Doppler broadening are present, the line profile is given by their convolution and is called the Voigt profile.

4.2.2 Free − bound transitions

These are the processes of photorecombination and photoionization. For photoionization from state k, the photon energy $h\nu \geq \varepsilon_{k\lambda}$ and the effective cross section $Q^{(k\to\lambda)} \sim \nu^{-3}$ must be present. The source of photorecombination radiation is given by the relation

$$j_\nu \sim \exp\left(-\frac{h\nu - \varepsilon_{k\lambda}}{k_b T_e}\right) \qquad \text{pro } h\nu \geq \varepsilon_{k\lambda} \ \text{ a } \ j_\nu = 0 \ \text{ pro } h\nu < \varepsilon_{k\lambda}$$

with a classical coefficient modified by the Gaunt factor g_{bf} depending on the emitting ion and the state into which the ion recombines. A jump called the recombination edge appears in the spectrum. This jump is blurred by all the mechanisms described for line broadening.

4.2.3 Free – free transitions

These are bremsstrahlung and collisional absorption. The spectrum of bremsstrahlung is close to $\sim \exp(-h\nu/k_B T_e)$. The total power is

$$P^{ff} \sim Z^2 n_e n_i T_e^{1/2} \overline{g}_{ff} \ ,$$

where Z is the charge of the ion and $\overline{g}_{ff}$ is the Gaunt factor for bremsstrahlung. We see that the bremsstrahlung power is proportional to the square root of the electron temperature. It therefore increases with temperature much more slowly than the power radiated by a blackbody. The ratio between the power radiated by recombination to state k and the bremsstrahlung is [3]

$$\frac{P_k^{fb}}{P^{ff}} \simeq \frac{2\varepsilon_{k\lambda}/k}{k_B T_e} \quad ,$$

where k for the hydrogen-like ion is the principal quantum number. The effective cross section for the collisional absorption of a photon is

$$Q_\nu^{ff} \sim \frac{n_e n_i Z^2 \overline{g}_{ff}}{\nu^3 v_{Te}}$$

We will also mention cyclotron radiation, which is also a free-to-free transition, although it is not an atomic process, but rather the emission of a free electron when moving in a magnetic field. The electron moves with acceleration when gyrating around a magnetic field line, and therefore radiates mainly at the electron cyclotron frequency ω_{ce} and also at its integer multiples (harmonic frequencies). The power emitted by an electron is given by the relation

$$P = \frac{e^2}{4\pi\varepsilon_0} \ \frac{4\omega_{ce}^2}{3 m_e c^2} \ \frac{8\pi}{3} \ E_{kin} \ ,$$

where E_{kin} is the kinetic energy of the electron. The kinetic energy of the electron therefore decreases exponentially over time. For a magnetic field of 1 T, the electron cyclotron frequency is $\omega_{ce} = 1.76 \times 10^{11}$ s^{-1} and the characteristic time of the electron energy decay is about 0.3 s.

4.2.4 Radiation Transport

We will describe the transport of radiation at a frequency much higher than the plasma frequency. In this case, the relative permittivity of the plasma is approximately 1 and the group velocity of radiation is approximately equal to the speed of light in vacuum. Then the transport of radiation along the beam path l is described by the following equation for the spectral intensity I_ν

$$\frac{1}{c}\frac{\partial I_\nu}{\partial t} + \frac{\partial I_\nu}{\partial l} = j_\nu - k_\nu I_\nu \ , \tag{29}$$

where j_ν is the spectral density of the power radiated by spontaneous emission from a unit volume and k_ν is the effective absorption coefficient, which is the absorption coefficient minus the stimulated emission coefficient (k_ν is negative, if lasing occurs at a given frequency). The

quantities j_ν, k_ν may depend on the direction $\vec{\Omega}$ of radiation propagation, for example, due to a non-zero ion flow velocity. In the equation (29), scattering of radiation is neglected for simplicity.

Let L be the characteristic dimension of the plasma. If $k_\nu L \ll 1$, we say that the plasma is **optically thin** for a given frequency. Almost every photon emitted in an optically thin plasma escapes from it. Laboratory plasmas are often optically thin except for the frequencies of the strongest lines. If, on the other hand, $k_\nu L \gg 1$, we say that the plasma is **optically thick** for a given frequency. Photons emitted deep in an optically thick plasma are reabsorbed in the plasma and have only a very small chance of reaching its surface. Magnetically confined plasma is usually optically thick for cyclotron radiation at the frequency ω_{ce}, for a magnetic field of 1 T and an electron density of 10^{19} m^{-3}, the attenuation length is about 12 μm.A blackbody is optically thick for all frequencies.

5 Population (occupancy) of individual states

The population of individual states (the number of ions in a given state per unit volume) can be calculated either using various analytical approximations or by solving rate equations.

5.1 Thermodynamic equilibrium (TE)

Thermodynamic equilibrium can be characterized by the following four conditions.

1. The radiation spectrum corresponds to the Planck spectrum of a blackbody

$$B_\nu = \frac{2h\nu^3/c^2}{\mathrm{e}^{h\nu/k_BT} - 1} \ . \tag{30}$$

2. The velocity distribution of ions and free electrons is Maxwellian with temperature T (the temperatures of electrons, ions, and radiation are equal $T_e = T_i = T_r = T$).

3. The equilibrium between the excited states of ions of the same degree of ionization is given by the Boltzmann relation

$$\frac{n_l}{n_k} = \frac{g_l}{g_k}\mathrm{e}^{-\varepsilon_{kl}/k_BT} \ , \tag{31}$$

where g are the degeneracies of the given states and $\varepsilon_{kl} = \varepsilon_l - \varepsilon_k$ is the difference in the energies of the given states.

The ratio of the sum of populations n to the population n_1 of the ground state is given by

$$\frac{n}{n_1} = \sum_{k=1}^{k_{max}} \frac{n_k}{n_1} = \frac{1}{g_1}\sum_{k=1}^{k_{max}} g_k \mathrm{e}^{-\varepsilon_k/k_BT} = \frac{Z(T)}{g_1} \ .$$

Note that the partition function $Z(T)$ diverges for $k_{max} = \infty$. However, it should be noted that for high states the radius of the orbit of the outer electron of an isolated ion will be larger than the average distance to the nearest ion. Such states are not states of an isolated ion, they are influenced by the environment and may not be bound. The influence of the environment will be manifested by a decrease in the ionization potential ΔI, which will also be reflected in the emission spectrum by a shift of the recombination edge and the absence of lines corresponding to high-energy states. In the simplest approximation, it

can be assumed that states with energy higher than $I_p - \Delta I$ are not bound. If the energy ε_2 of the first excited state is much greater than the thermal energy $k_B T$, then $Z(T) \simeq g_1$ and the populations of excited states are very small compared to the population of the ground state.

4. Ionization equilibrium is actually a chemical equilibrium and is given by the Saha equation. We shall generally describe the equilibrium between ionization degrees p and $p+1$ (for a neutral atom $p = 0$). The partition function for a free electron is

$$Z_e = 2\left(\frac{2\pi m_e k_B T_e}{h^2}\right)^{3/2} .$$

For the population $n_{k,p}$ of the k-th excited state of ionization degree p and the population $n_{1,p+1}$ of the ground state of ionization degree $p+1$,

$$\frac{n_e n_{1,p+1}}{n_{k,p}} = 2\frac{g_{1,p+1}}{g_{k,p}}\left(\frac{2\pi m_e k_B T_e}{h^2}\right)^{3/2} \exp\left(-\frac{\varepsilon_{k\lambda}}{k_B T_e}\right) .$$

For the total populations of ionization states, then,

$$\frac{n_e n_{p+1}}{n_p} = 2\frac{Z_{p+1}}{Z_p}\left(\frac{2\pi m_e k_B T_e}{h^2}\right)^{3/2} \exp\left(-\frac{I_p}{k_B T_e}\right) , \tag{32}$$

where the partition functions Z_{p+1}, Z_p are given by the partition functions of the excitation states, since the partition functions of the translational motion differ negligibly.

5.2 Local thermodynamic equilibrium (LTE)

The radiation spectrum in laboratory plasma is usually dominated by narrow spectral features (spectral lines and recombination edges), and the spectrum thus differs significantly from the radiation of a blackbody.

In LTE, the matter is in equilibrium, but the radiation is not. Maxwell's distribution for electrons, the Boltzmann relation between the populations of excitation levels, and the Saha equation apply. Such a situation is possible in dense plasmas, when collisional processes everywhere prevail over radiative processes influenced by the radiation spectrum (photoexcitation, photoionization, and stimulated emission).

If the influence of the radiation spectrum on the populations of states can be neglected, then the populations are determined by local conditions at a given location, which is why we speak of LTE.

5.3 Coronal equilibrium (CE)

This is a stationary state in a very dilute plasma, where neglecting slow processes greatly simplifies the calculation of populations. In a very dilute plasma, collisional deexcitation can be neglected against photodeexcitation, and three-particle and dielectron recombination can be neglected against photorecombination.

5.4 Collisional-radiative model

We solve the rate equations for populations of excited states of different ionization degrees. At each location we obtain a system of ordinary differential equations. If we are looking for a stationary state, we set the right-hand sides equal to 0.

The coupling between different locations is given only by the transport of radiation. In the optically thin plasma approximation, the effect of the radiation spectrum on the populations can be neglected and the populations can then be solved locally (for each Lagrangian cell separately).

5.5 Principle of detailed balancing

In equilibrium, the differential reaction rates of the direct and inverse processes must be the same (invariance to time reversal). From the differential cross section of the direct process, the differential cross section of the inverse process can be calculated, and it can be used outside of equilibrium.

If I also consider the Maxwell distribution of electrons outside of equilibrium, the same procedure can be applied to the rate coefficients. In equilibrium, the collision excitation rate is equal to the collision deexcitation rate, and the collision ionization rate is equal to the three-particle recombination rate. From the rate coefficient of the direct process, the rate coefficient of the inverse process can be calculated, and it can be used outside of equilibrium. One application of the principle of detailed balancing is the relations between the Einstein coefficients. Calculating coefficients from detailed balancing is also advantageous for numerical modeling, because the preservation of the equilibrium solution is automatically guaranteed.

References

[1] T. Ohlsson. *Relativistic Quantum Physics: From Advanced Quantum Mechanics to Introductory Quantum Field Theory.* Cambridge University Press, Cambridge 2011.

[2] R.D. Cowan. *Theory of atomic structure and spectra.* University of California Press, Berkeley 1981.

[3] M. Mitchner and C.H. Kruger, Jr. *Partially Ionized Gases.* J. Wiley & Sons, 1973.